MDAG.com Internet Case Study 41

Nonlinear Science of Minesite-Drainage Chemistry.
1 - Scaling and Buffering

by K.A. Morin

© 2015   Kevin A. Morin

www.mdag.com/case_studies/cs41.html

Abstract

This MDAG case study discusses two examples of nonlinearity in minesite-drainage chemistry: scaling and buffering. These nonlinear aspects show that complexity can lead to unexpected trends and that cause and effect are not often proportional.

The first example is scaling, in which aqueous concentrations in each liter of drainage water increase as other conditions increase, such as scale, weight, time, solid:liquid ratio, reaction rate, residence time, and distance along flowpath. However, aqueous concentrations in a liter of water cannot increase limitlessly, so at some point the "scale transition" is crossed and concentrations stabilize within narrow "equilibrium" ranges. At near-neutral pH, this can happen for copper with as little as 40 kg or as much as 40 tonnes of rock or tailings, or over flowpath lengths of 2 cm to 20 m for rock or tailings.

Therefore, upon increasing beyond relatively small scales, there is a change to nonlinear conditions, where aqueous concentrations do not increase proportionally to increases in scale. This realization contradicts the typical approach of using scaling factors from laboratory-based kinetic tests to predict full-scale minesite concentrations.

The second nonlinear example in drainage chemistry is aqueous buffering, where pH and pH-dependent aqueous concentrations remain relatively stable upon the addition of dilute drainage or the addition of acidic or alkaline drainage. There are two primary sources of pH buffering for minesite drainage: aqueous reactions within the water and solid-liquid interactions.

The first buffering source is illustrated by the conversion of aqueous species such as bicarbonate to/from carbonate and carbonic acid. This aqueous conversion of bicarbonate can maintain pH around 6.4 or 10.3 at $25^{\circ}C$.

The second source by far provides the greater buffering at full-scale minesites, where even trace amounts of mineral groups can regulate pH and aqueous chemistry for extended times and distances. Aqueous buffering by solid-phase mineral groups can lead to chromatographic-like, step-like changes in aqueous pH and concentrations through time and distance, with each step called a geochemical "sub-region". In fact, a particular range of observed pH at a minesite can often reveal the mineral group accounting for this buffered pH and associated chemistry. This was shown by field studies and computer simulations in the early 1980's and by full-scale bimodal pH distributions

at minesites.

Mass-balance simulations show interesting nonlinear characteristics of geochemical sub-regions. For example, downgradient boundaries migrate faster than upgradient boundaries, and thus the lengths of sub-regions stretch with increasing time. Nonetheless, the downstream pH does not fall immediately to the most acidic, input value.

1. INTRODUCTION

Because minesite-drainage chemistry is called a "nonlinear science" in this MDAG case study, a simple question is: what is a nonlinear science?

> "When asked this question at a cocktail party, I often paraphrase Aristotle, saying that nonlinear science is the study of those dynamic phenomena for which the whole differs from the sum of its parts . . . which is in some sense a metascience with roots reaching into widely diverse areas of modern research." (Scott, 2007)

The words, "the whole differs from the sum of its parts", harken back a quarter century before that quotation, to the "broken symmetry of science" discussed by Anderson (1972):

> "The constructionist hypothesis breaks down when confronted with the twin difficulties of scale and complexity. . . . At each level of complexity entirely new properties appear . . . We can now see that the whole becomes not merely more, but very different from the sum of its parts."

On nonlinear science, Wikipedia (2015) adds:

> "In physics and other sciences, a nonlinear system, in contrast to a linear system, is a system which does not satisfy the superposition principle – meaning that the output of a nonlinear system is not directly proportional to the input. . . . Nonlinear problems are of interest to engineers, physicists and mathematicians and many other scientists because most systems are inherently nonlinear in nature. . . . [S]ome aspects of the behavior of a nonlinear system appear commonly to be chaotic, unpredictable or counterintuitive. Although such chaotic behavior may resemble random behavior, it is absolutely not random."

Therefore, a nonlinear science is complex, with cause and effect not proportional and not always apparent. To me, this applies to all sciences in some way or another. This MDAG case study is the first in a series to discuss nonlinear aspects of minesite-drainage chemistry, focussing on (a) scaling and (b) aqueous buffering.

2. SCALING

We have already written a great deal on scaling up minesite-drainage chemistry from micropore spaces to typical laboratory-based tests to full-scale minesite components (Morin and Hutt, 2007; Morin, 2014 and 2015). This work showed, for all scales, that physical aspects like water flowpaths, sequences of minerals, and sampling location can affect drainage chemistry. One example on the microscale of pores showed how variable chemistry could be over short distances, and that various averaged concentrations and rates over the pore network did not agree. Also, acid-base accounting and laboratory kinetic tests on a larger scale implicitly predict homogenized conditions, which do not apply to full-scale minesite components.

As scale increases, at some point a "scale transition" arises, representing the general break between kinetically determined (more-or-less linear with scale) and equilibrium determined (scale independent) concentrations in mg/L. In this case, "equilibrium" encompasses mechanisms such as thermodynamic equilibrium, metastable equilibrium, dynamic equilibrium, pseudo-equilibrium, and emergence. Emergence can generally be defined as the appearance of distinct patterns or properties as scale increases, due to self-organization in complex systems, or "the whole becomes not merely more, but very different from the sum of its parts" (Anderson, 1972).

Examples showed that the scale transition for near-neutral copper leaching could require as little as 40 kg, or as much as 40 tonnes of rock or tailings. These weights translated into flowpath lengths of 2 cm to 20 m for rock or tailings. This shows that the scale transition should often be encountered within full-scale minesite components, but not necessarily in small-scale on-site test components (such as one-tonne rock piles) or laboratory-based laboratory testwork (such as 1 kg humidity cells).

The scale transition is the first example in this MDAG case study of nonlinear minesite-drainage chemistry. It can be shown graphically (Figure 1), and derives from two basic observations:
  1) As the properties on the x-axis in Figure 1, starting at the origin, increase in value, each liter of water collects additional mg/L on the y-axis.
  2) Because a liter will not accumulate a limitless number of mg/L, the accumulation must stop at some narrow range of equilibrium concentration.

This is re-depicted in Figure 2, showing the various scales of minesite-drainage testwork and how some cross the scale transition.

This issue is particularly important because of the current standard technique for predicting minesite-drainage chemistry. The standard involves deriving a "scaling factor" based on arbitrary selections from small-scale testwork, and applying this factor to full-scale minesite components linearly with full-scale weight and flow rates (Morin, 2014). Figures 1 and 2 are sufficient to show this is inappropriate where the scale transition is exceeded. This happens, for copper, at near-neutral pH with as little as 40 kg of material or 2 cm of flowpath.
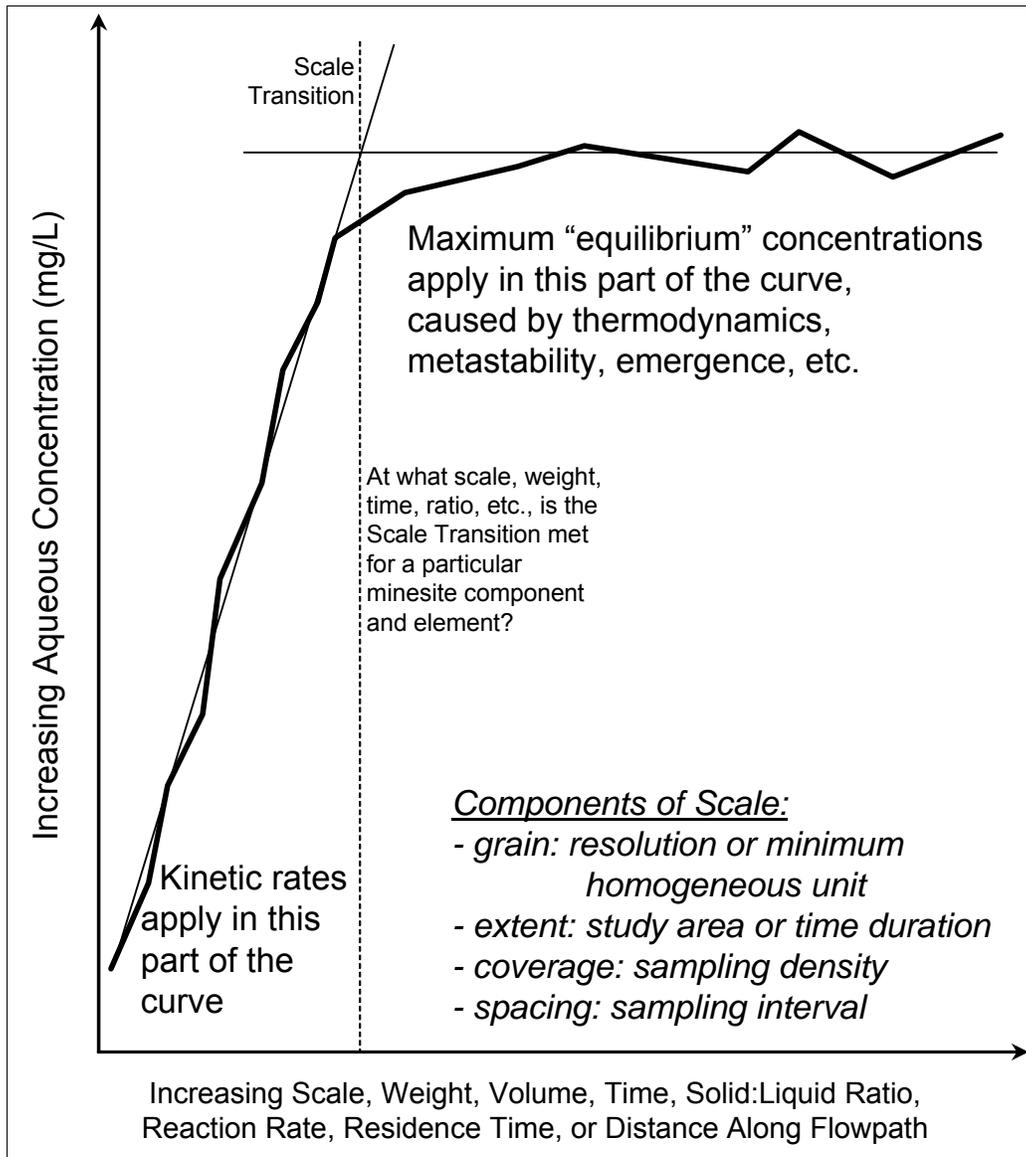
The graph shows "Increasing Aqueous Concentration (mg/L)" on the y-axis and "Increasing Scale, Weight, Volume, Time, Solid:Liquid Ratio, Reaction Rate, Residence Time, or Distance Along Flowpath" on the x-axis.

Labels within the figure:
- Scale Transition
- Maximum "equilibrium" concentrations apply in this part of the curve, caused by thermodynamics, metastability, emergence, etc.
- At what scale, weight, time, ratio, etc., is the Scale Transition met for a particular minesite component and element?
- Kinetic rates apply in this part of the curve
- *Components of Scale:*
  - *- grain: resolution or minimum homogeneous unit*
  - *- extent: study area or time duration*
  - *- coverage: sampling density*
  - *- spacing: sampling interval*

Figure 1. The conceptual model for scaling minesite-drainage chemistry through kinetic and equilibrium conditions, including components of scale.
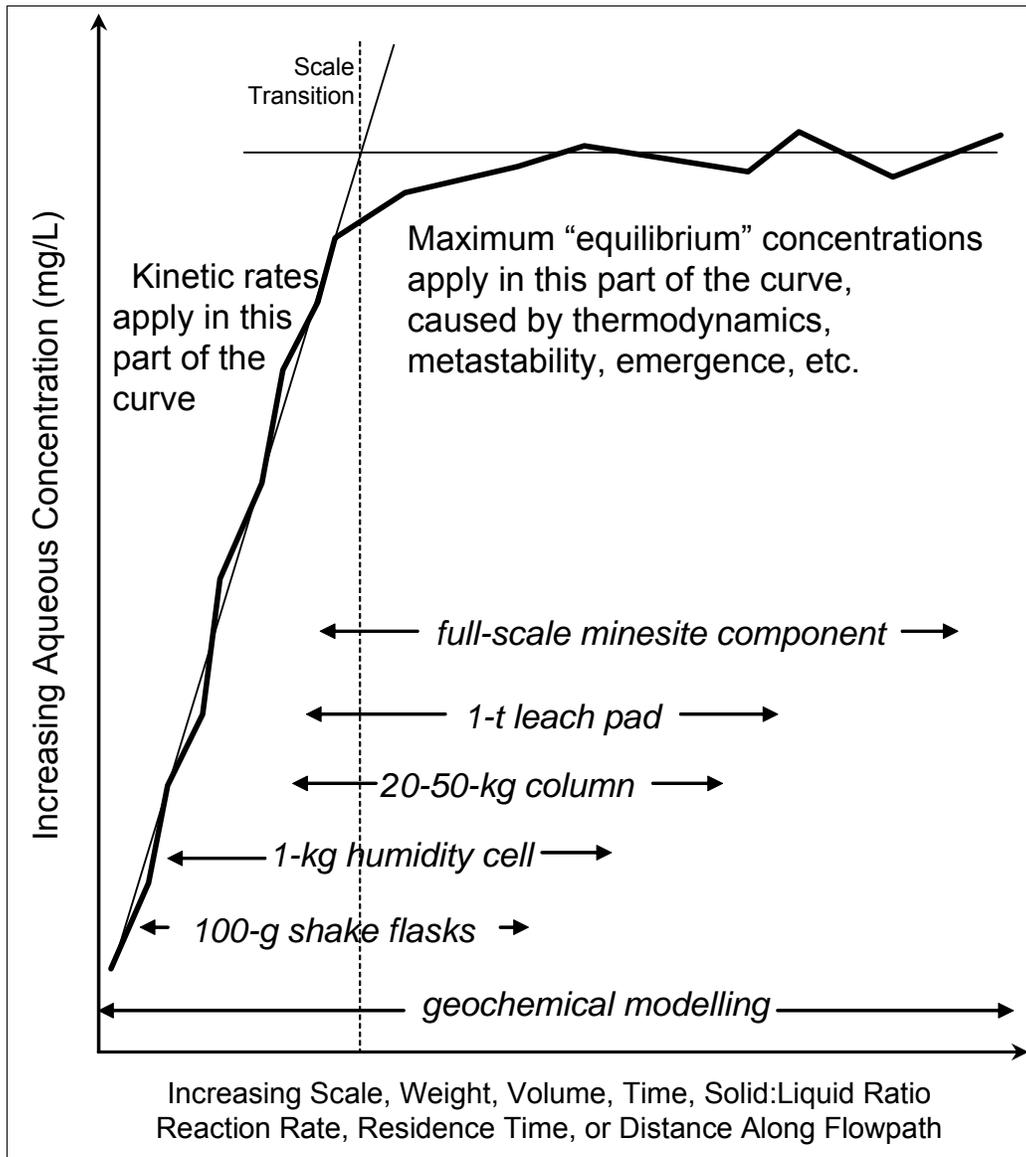
Scale
Transition

Increasing Aqueous Concentration (mg/L)

Kinetic rates
apply in this
part of the
curve

Maximum "equilibrium" concentrations
apply in this part of the curve,
caused by thermodynamics,
metastability, emergence, etc.

full-scale minesite component

1-t leach pad

20-50-kg column

1-kg humidity cell

100-g shake flasks

geochemical modelling

Increasing Scale, Weight, Volume, Time, Solid:Liquid Ratio
Reaction Rate, Residence Time, or Distance Along Flowpath

Figure 2. The conceptual model for scaling minesite-drainage chemistry, with general ranges of scale for various types of geochemical testwork and models.
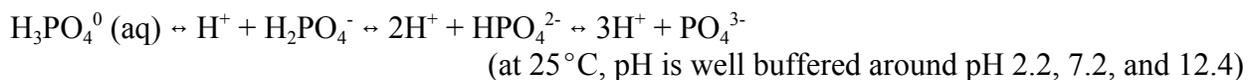
3. BUFFERING

The second nonlinear aspect of minesite-drainage chemistry discussed in this MDAG case study is buffering. In a general sense, the main feature of aqueous buffering is the regulation of aqueous pH, that is, a nearly constant pH is maintained if the drainage is diluted, or if relatively small amounts of more acidic or more alkaline drainages are added. In other words, buffered minesite drainages resist pH changes in nonlinear ways (Figure 3). This can lead to bimodal distributions at minesites that have drainages in more than one pH range (e.g., Morin and Hutt, 1997, 2001, and 2008).

"Buffering capacity" quantifies this resistance of pH to change at various values of pH (e.g., Michalowska-Kaczmarczyk and Michalowski, 2015). When redox (Eh) buffering capacity is considered with pH buffering capacity, a wavy two-dimensional surface (pH and Eh on the axes), unique to each water chemistry, shows the strong buffering points as "depressions" or "valleys" where the combination of pH and Eh tend to cluster. This accounts for full-scale observations at minesites, like bimodal pH distributions (Morin and Hutt, 2008) and close linkages between pH and Eh (Morin et al., 1982).

However, there is much more to this story than just control of pH (and Eh). Because aqueous concentrations and kinetic rates can be affected by pH, the buffering of pH leads to the buffering of some aqueous concentrations. In terms of Figures 1 and 2 above, pH can affect the magnitude of the equilibrium concentration on the y-axis and the point on the x-axis where the scale transition is crossed.

There are two primary sources of pH buffering for minesite drainage: aqueous reactions within the water and solid-liquid interactions.

Examples of buffering reactions within water are:

$H_2CO_3^0$ (aq) $\leftrightarrow$ H^+ + HCO_3^- $\leftrightarrow$ $2H^+$ + CO_3^{2-} (at 25°C, pH is well buffered around pH 6.4 and 10.3)

$H_3PO_4^0$ (aq) $\leftrightarrow$ H^+ + $H_2PO_4^-$ $\leftrightarrow$ $2H^+$ + HPO_4^{2-} $\leftrightarrow$ $3H^+$ + PO_4^{3-}
$\qquad\qquad\qquad$ (at 25°C, pH is well buffered around pH 2.2, 7.2, and 12.4)

$M(OH)_3$ $\leftrightarrow$ $M(OH)_2^+$ + OH^- $\leftrightarrow$ MOH^{+2} + $2OH^-$ $\leftrightarrow$ M^{+3} + $3OH^-$
$\qquad\qquad\qquad$ (where M represents a trivalent metal undergoing hydrolysis,
$\qquad\qquad\qquad$ which often leads to solid-liquid buffering discussed below)
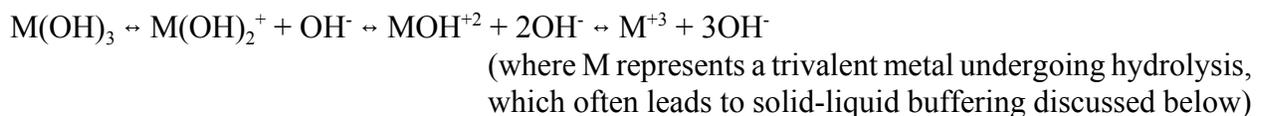
The second, and often by the far the greater, source of pH buffering for minesite drainage is solid-liquid interactions. While not obvious, even trace amounts of solid-phase minerals can produce strong aqueous buffering (Morin and Cherry, 1984).

As a simple numerical example, 1 m^3 of waste or tailings with a specific gravity of 3 and a saturated porosity of 35% contains 1.95 tonnes of solids and 350 L of water. If a mineral occurs at a trace level of 0.01%, the full dissolution of this trace amount into the 350 L can produce a maximum aqueous level of roughly 560 mg/L.
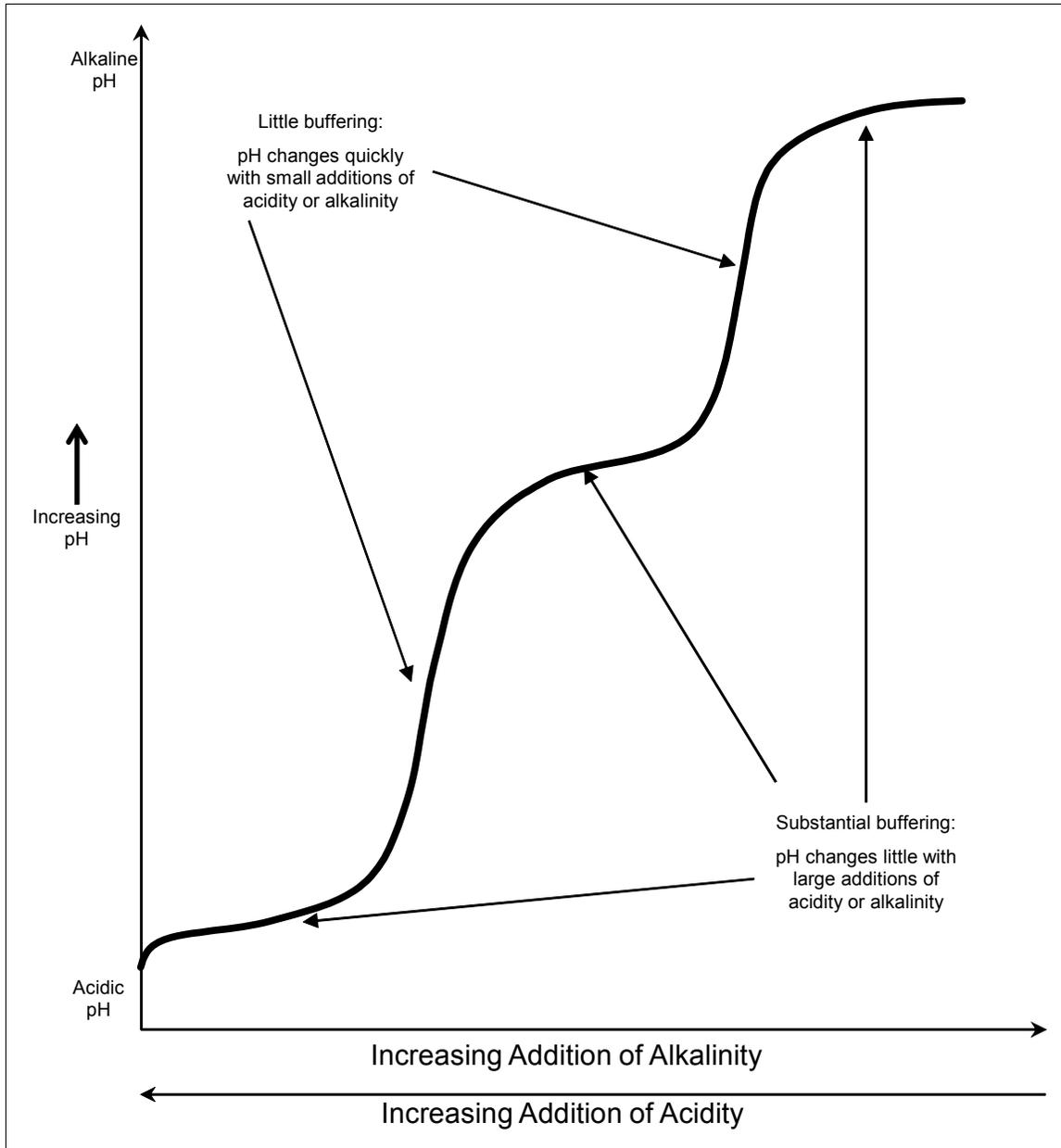
Figure 3. A simplified example of pH buffering, with pH increasing (upwards on the y-axis) nonlinearly as alkalinity is added (rightwards on the x-axis), or with pH decreasing (downwards on the y-axis) nonlinearly as acidity is added (leftwards on the x-axis).

Therefore, even a trace solid-phase amount of only 0.01% can exert a strong buffering effect on the drainage chemistry, which can persist for long times depending on water flowrates and dissolution rates. Because pH-buffering minerals like calcite often occur at higher levels (or at least are only detectable at higher levels), their buffering effects can be even more significant.

Morin et al. (1982) and Morin (1983) described and simulated chromatographic-like, almost step-like intermediate pH values in a ground water plume of ARD moving through a sand aquifer initially containing calcite (schematically depicted in Figure 4). These steps were called geochemical "sub-regions" of distinct mineral/mineral-group precipitation-dissolution (Table 1), reflecting transient equilibrium conditions (Morin et al., 1982; Morin, 1983; Morin et al., 1988a and 1988b; Morin and Cherry 1988). The lowest, persistent, acidic pH represented the "inner core" as the source of acidity, which eventually created the downgradient sub-regions in a sequence. A pseudo-three-dimensional schematic diagram depicts these geochemical sub-regions, where the axes are distance along flowpath and time (Figure 5).

This sub-region approach can also be applied to the input of alkaline water to a neutralizing flow system (Figure 6).

In effect, these geochemical sub-regions in Table 1 are elaborations on the earlier concept of abrasion pH in low-salinity water (Steven and Carron, 1948, and Grant, 1969; see also Table 2). However, abrasion pH does not address more complex conditions, like the ongoing input of acidic or alkaline water chemistry and the evolution of water chemistry through time.

According to mass-balance simulations (Morin, 1983), downgradient boundaries of geochemical sub-regions migrate faster than the upgradient boundaries. Thus, the lengths of the sub-regions stretch with increasing time (Figures 4, 5, and 6), but notably the downstream pH does not fall immediately to the most acidic, input value.

Based on Figures 4 to 6 and Table 1, a minesite with a long-term, persistent acidic pH of 4.0-4.5 probably reflects Al-OH solid-liquid buffering and the Al-OH sub-region. In contrast, a minesite with a more acidic range, around pH 3.0-3.5, probably reflects Fe-OH solid-liquid buffering. However, this second minesite would have had short-term, transient, higher pH values in the Al-OH sub-region which was eventually consumed by the ongoing input of acidity. In both cases, the question arises: will the observed, buffered pH persist indefinitely, or eventually be replaced by a lower pH. This can be answered by field studies and mass-balance calculations (Morin, 1983, Morin and Cherry, 1988, and Morin et al., 1988a and 1988b).

These geochemical sub-regions, and the buffering of pH and aqueous concentrations associated with them, are not rare or unusual, although not often seen as distinct stepwise changes. For example, they have been seen in increasing acidification of surface reservoirs (Cánovas et al., 2016), and in small-scale on-site rock piles like those recently at the Diavik Diamond Minesite in Canada (Sinclair, 2014; Bailey et al., 2016). Also, Jurjovec et al., (1995) noted sequential pH sub-regions in effluents from laboratory-based tailings columns caused by influent diluted sulphuric acid. Based on 64 acidic minesites discharges, some persisting for more than a century, Sánchez España et al. (2005) characterized pH ranges corresponding to precipitation-dissolution of specific mineral groups, which can be complex (Sánchez España et al., 2015).
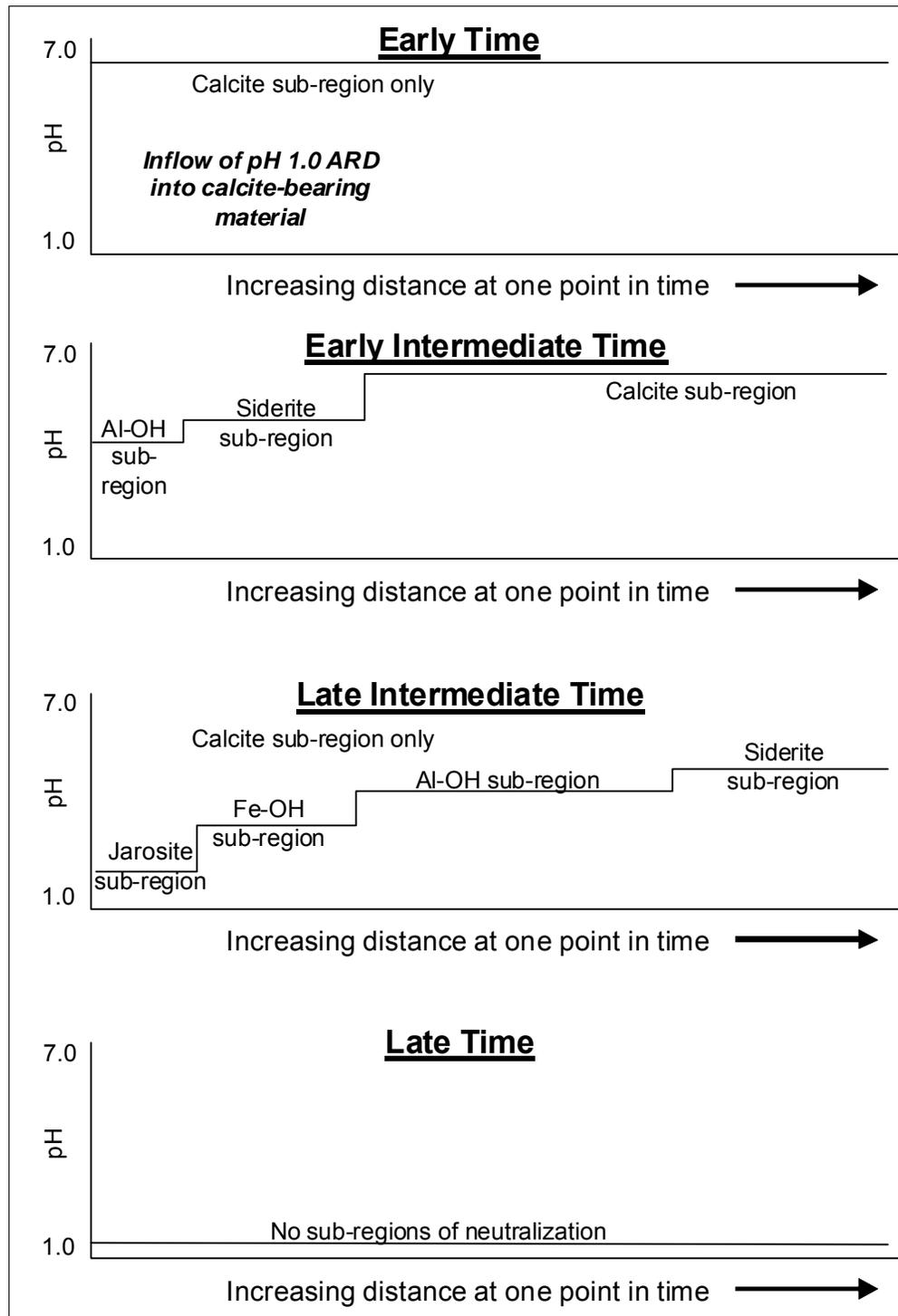
Figure 4. Schematic spatial movement and increasing size of geochemical sub-regions during input of pH 1.0 ARD into calcite-bearing material (based on Morin et al., 1982, and Morin, 1983).
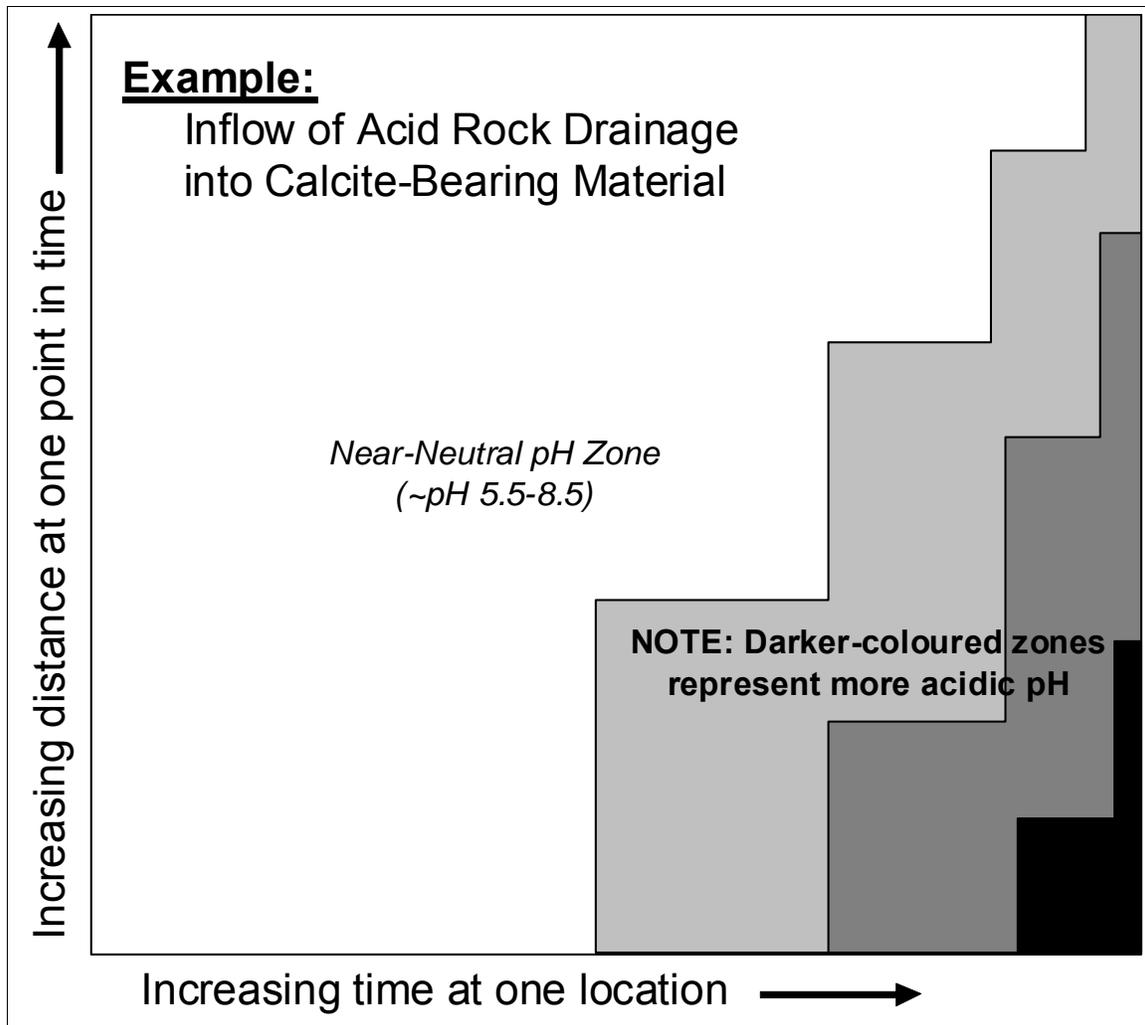
Figure 5. Pseudo-three-dimensional schematic diagram of the geochemical sub-region concept for an input of acidic water.

Table 1. Examples of equilibrium pH within geochemical sub-regions (compiled from data and references in Morin et al., 1982; Morin, 1983; Section 4.5 of Morin and Hutt, 1997 and 2001; Morin and Cherry, 1988; and Jurjovec et al., 1995)

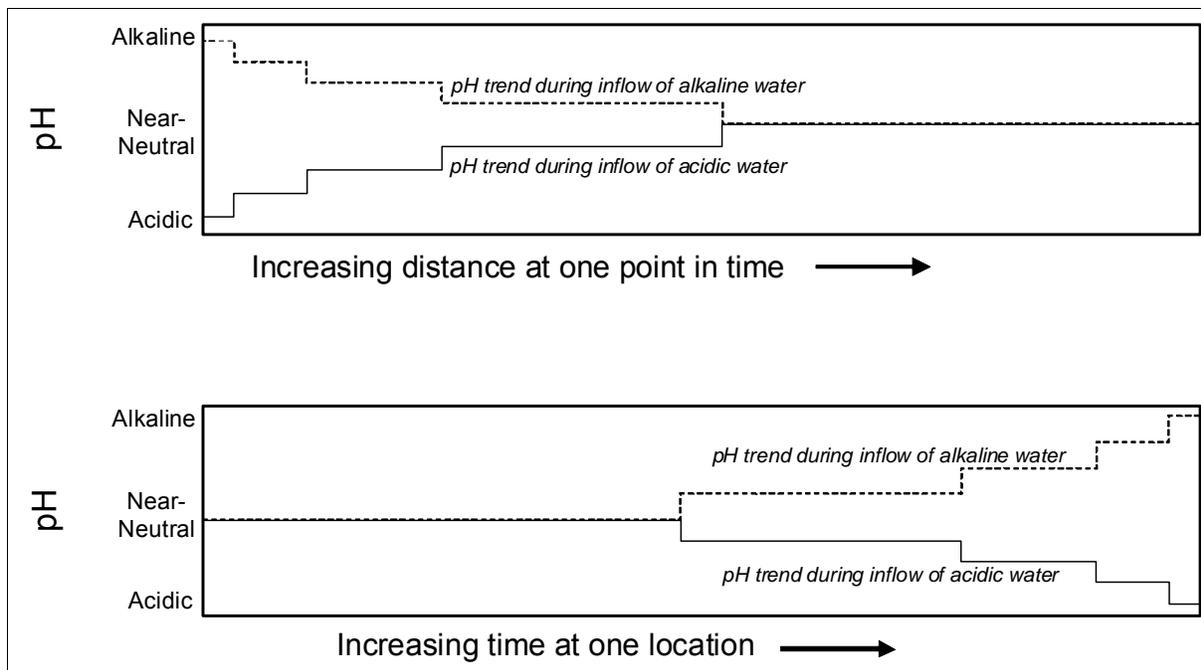| Dominant Mineral Controlling pH	General pH Range
Aluminosilicates	1.3
Jarosites	1.8
Fe-OH (where ferric iron is remobilized and rusty ferric-iron staining can become prominent)	3.0-3.7
Al-OH (white mineral staining can become prominent, but can be confused with gypsum)	4.3-5.0
Siderite (where ferrous iron is stable)	5.1-6.0
Calcite and related carbonates	5.5-8.5
Ion exchange	6.0-8.0
Brucite	10-11
Lime	12-13

Figure 6. Schematic diagrams of the geochemical sub-region concept at both increasing distances and increasing times, for inputs of acidic or alkaline water.

Table 2. Abrasion pH for various minerals (From Stevens and Carron, 1948)														
	Composition		Abrasion pH											
			Acidic						Neutral		Alkaline			
Mineral	Formula	Type[1]	1	2	3	4	5	6	7	8	9	10	11	12
Coquimbite	$Fe_2(SO_4)_3 \cdot 9H_2O$	b A	■											
Alunogen	$Al_2(SO_4)_3 \cdot 16H_2O$	b A		■										
Pickeringite	$MgAl_2(SO_4)_4 \cdot 22H_2O$	B b A			■									
Potash Alum	$KAl(SO_4)_2 \cdot 12H_2O$	B b A			■									
Aluminite	$Al_2SO_4 \cdot 9H_2O$	b A				■								
Scorodite	$FeAsO_4 \cdot 2H_2O$	b A					■							
Sessolite	H_3BO_3	a						■						
Jarosite	$K_2Fe_6(OH)_{12}(SO_4)_4$	b a						■						
Siderite	$FeCO_3$	b a						■	■					
Gypsum	$CaSO_4 \cdot 2H_2O$	B a							■					
Pyrophyillite	$Al_2Si_4O_{10}(OH)_2$	b a							■					
Quartz	SiO_2	a						■	■					
Gibbsite	$Al(OH)_3$	b						■						
Andalusite	Al_2SiO_5	b a							■					
Muscovite	$KAl_3Si_3O_{10}(OH)_2$	B b a							■					
Calcite	$CaCO_3$	B a								■				
Anorthite	$CaAl_2Si_2O_8$	B b a								■				
Microcline	$KAlSi_3O_8$	B b a								■	■			
Talc	$Mg_3Si_4O_{10}(OH)_2$	B a									■			
Albite	$NaAlSi_3O_8$	B b a									■	■		
Dolomite	$CaMg(CO_3)_2$	B B a									■	■		
Borax	$Na_2B_4O_7 \cdot 10H_2O$	B a									■			
Phlogopite	$KMg_3AlSi_3O_{10}(OH)_2$	B B b a										■	■	
Magnesite	$MgCO_3$	B a										■		
Brucite	$Mg(OH)_2$	B											■	
Merwinite	$Ca_3Mg(SiO_4)_2$	B B a										■		
Shertite	$Na_2Ca_2(CO_3)_3$	B B a												■

[1] A = strong acid   B = strong base   a = weak acid   b = weak base

4. CONCLUSION

This MDAG case study discussed two examples of nonlinearity in minesite-drainage chemistry: scaling and buffering. These nonlinear aspects show that complexity can lead to unexpected trends and that cause and effect are not often proportional.

Nonlinear aspects of scaling are attributable to exceeding the scale transition at relatively small scales. As a result, there is a change from kinetic (more-or-less linear) or equilibrium (nonlinear with scale) conditions.

Nonlinear aspects of buffering are attributable to aqueous and solid-liquid interactions that restrict pH and pH-dependent aqueous concentrations to narrow ranges. These ranges are overcome only with significant additions of more acidic or more alkaline drainages. Due to solid-liquid buffering, pH does not change drastically in one step, but in chromatographic-like stepwise progressions, called geochemical sub-regions, occurring with distance and time. Field studies and simulations from the early 1980's showed a significantly nonlinear but predictable behaviour to the sub-regions. In fact, the measured pH of a sub-region can often reveal the solid-phase mineral group accounting for that pH and ongoing buffering.

5. REFERENCES

Anderson, P.W. 1972. More is different: Broken symmetry and the nature of the hierarchical structure of science. Science 177, p. 393-396.

Bailey, B.L., D.W. Blowes, L. Smith, and D.C. Sego. 2016. The Diavik Waste Rock Project: Geochemical and microbiological characterization of low sulfide content large-scale waste rock test piles. Applied Geochemistry, 65, p. 54–72.

Cánovas, C.R., M. Olias, F. Macias, E. Torres, E.G. San Miguel, L. Galván, C. Ayora, and J.M. Nieto. 2016. Water acidification trends in a reservoir of the Iberian Pyrite Belt (SW Spain). Science of the Total Environment, 541, p. 400-411.

Grant, W.H. 1969. Abrasion pH, an Index of chemical weathering. Clays and Clay Minerals, 17, p. 151-155.

Jurjovec, J., D.W. Blowes, and C.J. Ptacek. 1995. Acid Neutralization in Mill Tailings and the Effect of Natrojarosite Addition. IN: T.P. Hynes and M.C. Blanchette, eds., Sudbury '95, Proceedings of the Conference on Mining and the Environment, Sudbury, Ontario, May 28 - June 1, Volume 1, p.29-38.

Michalowska-Kaczmarczyk, A.M. and T. Michalowski. 2015. Dynamic buffer capacity in acid-base systems. Journal of Solution Chemistry, 44, p. 1256-1266.

Morin, K.A. 2015. Fractal and Lognormal Characteristics, Short-Term Maximum Concentrations, and Appropriate Time Discretization of Minesite-Drainage Chemistry. MDAG Internet Case Study #40, www.mdag.com/case_studies/cs40.html

Morin, K.A. 2014. Applicability of scaling factors to humidity-cell kinetic rates for larger-scale predictions. IN: 21st Annual BC/MEND Metal Leaching/Acid Rock Drainage Workshop, Challenges and Best Practices in Metal Leaching and Acid Rock Drainage December 3-4, 2014, Simon Fraser University Harbour Centre, Vancouver, British Columbia, Canada.

Morin, K.A. 1983. Prediction Of Subsurface Contaminant Transport In Acidic Seepage From Uranium Tailings Impounds. Ph.D. Thesis, Department of Earth Sciences, University of Waterloo, Ontario. Supervisor: Dr. John A. Cherry.

Morin, K.A., and J.A. Cherry. 1988. Migration of acidic groundwater seepage from uranium-tailings impounds, 3. Simulation of the conceptual model with application to Seepage Area A. Journal of Contaminant Hydrology, 2, p.323-342.

Morin, K.A., and J.A. Cherry. 1986. Trace amounts of siderite near a uranium-tailings impoundment, Elliot Lake, Ontario, and its implication in controlling contaminant migration in a sand aquifer. Chemical Geology, 56, p.117-134.

Morin, K.A., and N.M. Hutt. 2008. Bimodal Distribution of pH at Minesites with Acid Rock Drainage. MDAG Internet Case Study #28, www.mdag.com/case_studies/cs28.html

Morin, K.A., and N.M. Hutt. 2007. Scaling and Equilibrium Concentrations in Minesite-Drainage Chemistry. MDAG Internet Case Study #26, www.mdag.com/case_studies/cs26.html

Morin, K.A., and N.M. Hutt. 2001. *Environmental Geochemistry of Minesite Drainage: Practical Theory and Case Studies, Digital Edition*. MDAG Publishing (www.mdag.com), Surrey, British Columbia. ISBN: 0-9682039-1-4.

Morin, K.A., and N.M. Hutt. 1997. *Environmental Geochemistry of Minesite Drainage: Practical Theory and Case Studies*. MDAG Publishing (www.mdag.com), Surrey, British Columbia. ISBN: 0-9682039-0-6.

Morin, K.A., J.A. Cherry, N.K. Davé, T.P. Lim, and A.J. Vivyurka. 1988a. Migration of acidic groundwater seepage from uranium-tailings impounds, 1. Field study and conceptual hydrogeochemical model. Journal of Contaminant Hydrology, 2, p.271-303.

Morin, K.A., J.A. Cherry, N.K. Davé, T.P. Lim, and A.J. Vivyurka. 1988b. Migration of acidic groundwater seepage from uranium-tailings impounds, 2. Geochemical behavior of radionuclides in groundwater. Journal of Contaminant Hydrology, 2, p.305-322.

Morin, K.A., J.A. Cherry, T.P. Lim, and A.J. Vivyurka. 1982. Contaminant migration in a sand aquifer near an inactive tailings impoundment, Elliot Lake, Ontario. Canadian Geotechnical Journal, 19, p.49-62.

Sánchez España, J., I. Yusta, J. Gray, and W.D. Burgos. 2015. Geochemistry of dissolved aluminum at low pH: Extent and significance of Al-Fe(III) coprecipitation below pH 4.0. Geochimica et Cosmochimica Acta, online in December 2015 and in press.

Sánchez España, J., E. López Pamo, E. Santofimia, O. Aduvire, J. Reyes, and D. Barettino. 2005. Acid mine drainage in the Iberian Pyrite Belt (Odiel river watershed, Huelva, SW Spain): Geochemistry, mineralogy, and environmental implications. Applied Geochemistry, 20, p. 1320-1356.

Scott, A.C. 2007. The Nonlinear Universe: Chaos, Emergence, Life. Springer.

Sinclair, S.A. 2014. Influence of Freeze-Thaw Dynamics and Spatial Contributions on Geochemical Loading from a Low Sulfide Waste-Rock Pile. Master of Science Thesis in Earth Sciences, University of Waterloo.

Stevens, R.E., and M.K. Carron. 1948. Simple field test for distinguishing minerals by abrasion pH. American Mineralogist, 33, p. 31-39.

Wikipedia.org. 2015. Nonlinear System. Accessed October 2015 at en.wikipedia.org/wiki/Nonlinear_system